

Benefits of the Star Grain Configuration for a Sounding Rocket

Steven D. Stein*

United States Air Force Academy Department of Astronautics, USAFA, CO, 80841

Given a particular propellant formulation, the performance of a solid rocket motor is due largely to two factors: first, its volumetric efficiency and second, its average pressure over the course of the burn. The problem with the internal burning tube grain design is not enough surface area exists at the beginning of the burn. This causes the pressure to rise to very high levels towards the end of the burn and creates a potential flow separation problem at start-up. Additionally, an internal burning tube design creates a progressive burn; which is exactly opposite of the ambient pressure curve for a sounding rocket trajectory, decreasing efficiency. Using a star design to add more initial burn area allows for greater start-up pressure and a more neutral-regressive burn; which follows the ambient pressure curve more precisely. Additionally, the star design increases volumetric efficiency; increasing total impulse. The additional initial burn area also keeps the pressure in the chamber at a constant level, which allows for a higher average pressure during the burn which increases efficiency. The star grain configuration will also increase the range of possible payloads a sounding rocket can carry. This discussion will present the advantages of using a star grain configuration to improve the Air Force Academy's sounding rocket's altitude performance.

Nomenclature

$L1$	= star parameter describing depth of star
$L2$	= star parameter describing width of star
Ls	= length of the star along the main propellant grain
W	= web (amount of propellant burned in the perpendicular direction)
m	= slope of a line
b	= y-intercept of a line
"n"	= the line designated "n" (line "1", "2", etc.)
θ_n	= angle between line "n" and y-axis
R	= radius of the grain (the point where the star attached itself)
A_{LS}	= area along the length of the star (present along the main propellant grain)
A_{tri}	= area of the triangle portion of the aft end of the star pattern
$A_{ellipse}$	= area of the ellipse portion of the aft end of the star pattern
θ	= arc length representing the area lost from the addition of a star pattern
%gone	= percentage of area lost from the addition of a star pattern
La	= length of the aft section of a double taper grain design
Ra	= radius of the aft section of a double taper grain design
R_{case}	= radius of the inside of the case
Isp	= specific impulse

I. Introduction

THE main goal of a star grain configuration is to add more initial surface area. An increase in initial surface area is highly desired for a variety of reasons. Some reasons are safety (flow separation), performance (Isp), and payload carrying capacity (max g's). However, increasing the initial burn area usually requires sacrificing propellant to expose more surface area. The star grain configuration will increase the initial burn area without sacrificing volumetric efficiency; and in some cases will actually increase the volumetric efficiency. The star design

* Cadet, Astronautical Engineering Department, PO Box 2626, USAF Academy, CO, 80841, AIAA Student Member

can also produce a neutral-regressive burn profile. As the star burns, its surface area decreases as the outer portion of the grain expands, exposing more surface area. This trade off results in a neutral burn profile. Combined with a double taper grain design, the later portion of the burn becomes regressive. The neutral-regressive burn is much more desirable when compared to a completely regressive burn profile. In the end, the star grain configuration will out-perform all grain designs not containing a star pattern.

II. Effects of Increasing Initial Burn Area

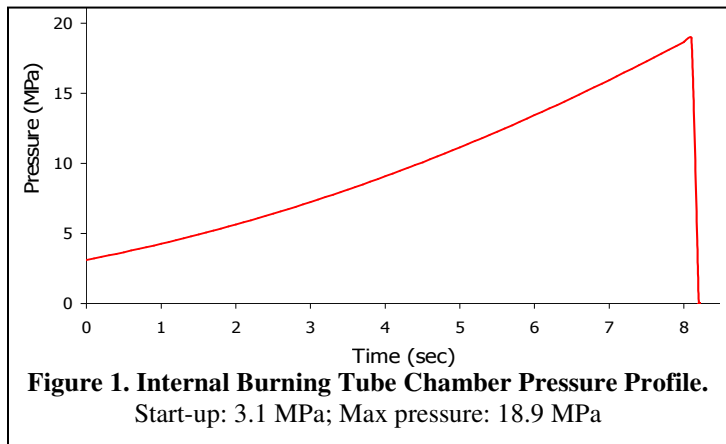
Low initial burn area can create many problems which can lead to total mission failure. A great example of a grain with low initial burn area is the internal burning tube grain.

A. Internal Burning Tube Grain Design

When using an internal burning tube design, there is little surface area available to produce pressure inside the case. This can lead to ignition problems and flow separation in the nozzle. For certain propellants, a minimum start-up pressure is required for a clean ignition. The propellant used in the FalconLAUNCH V program requires a start-up pressure of 3.1 MPa (450 psi). If an internal burning tube design is used with the FalconLAUNCH V propellant, the throat of the nozzle would have to be reduced significantly to account for this, causing pressure related problems. Additionally, there are nozzle concerns due to heating and throat erosion. Knowing the initial start-up pressure is fixed, the resulting maximum pressure is very high due to the progressive nature of the internal burning tube. Fig. 1 provides the pressure data for an internal burning tube design.

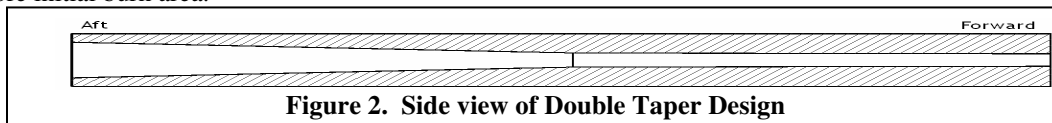
The maximum pressure for the internal burning tube design rises to very high levels. If the pressure is too high, the pressure vessel could crack or break resulting in total mission failure. Thus, the internal burning tube was not considered a viable option for the FalconLAUNCH program.

Another safety concern is flow separation in the nozzle. ¹In 1954, Summerfield performed a series of experiments analyzing flow separation in over expanded supersonic nozzles. Summerfield's experiments showed that as the ambient pressure increased with respect to the exit pressure, shockwaves present outside the nozzle would begin to move inside the nozzle. This does two things: the effective exit diameter becomes smaller and the shockwaves inside the nozzle could cause damage. In 1984, Oates, by analyzing Summerfield's experiments, discovered flow separation in the nozzle occurs when the ambient pressure is 2.5 - 3 times as large as the exit pressure. A good "rule of thumb" is to use 2.75 for this pressure ratio between ambient and exit pressure. This means that for a sea level launch (ambient pressure = 101.7 kPa) the exit pressure must be above 37 kPa to avoid flow separation. If a nozzle were designed to maximize the total impulse for a sea level launch using the internal burning tube design, the expansion ratio is about 13.4. Keeping in mind the start-up chamber pressure for this design is 3.1 MPa, the start-up exit pressure becomes 25.8 kPa. Because this number is below the 37 kPa threshold, flow separation will occur in the nozzle for the internal burning tube design. To avoid this problem, either the exit diameter would have to be decreased (decreasing efficiency), the start-up pressure would need to increase (increasing the already large maximum chamber pressure), and/or the launch needs to occur at a location higher than sea level (limiting the choice of launch locations).



B. Increasing Initial Burn Area

An increase in initial burn area facilitates the minimum startup pressure requirement. However, increasing the initial burn area without sacrificing volumetric efficiency is quite a challenge. Getting the burn area to stay nearly constant or decrease slightly over the course of the burn would provide optimum performance. The FalconLAUNCH program realized these problems. The solution proposed is a double taper grain design to allow for more initial burn area.



The aft section of the grain is enlarged with respect to the rest of the grain. This design achieves two important objectives: one, increasing the start-up pressure and, two, decreasing maximum pressure due to the higher initial burn area and lower maximum burn area. This eliminates both the flow separation and the maximum pressure problems present with the internal burning tube design. Fig. 3 shows the pressure profile for a double taper grain design using the same nozzle throat size as the internal burning tube grain design produced in Fig. 1.

The double taper design sacrifices total impulse and efficiency. The volumetric efficiency of a grain design corresponds to the total impulse produced by the rocket. The double taper gains an initial burn area increase by sacrificing propellant in the aft section. The loss in propellant results in a loss in total impulse. Additionally, the double taper design produces less average chamber pressure. Average chamber pressure is directly related to specific impulse (I_{sp}). Accounting for volume and efficiency losses, the loss in total impulse is quite drastic. Using the examples above, the total impulse of the double taper design is 6.5% less than the internal burning tube design. However, the double taper design is a more feasible option because of the significant drop in maximum chamber pressure due to pressure vessel restrictions.

An increase in initial burn area will prevent flow separation. Using the example found in Fig. 3, a nozzle optimized for maximum total impulse has an expansion ratio of 8.9. The initial exit pressure using an initial chamber pressure of 3.1 MPa is 44.6 kPa. The exit pressure is above the 37 kPa threshold needed to avoid flow separation in the nozzle.

Aside from flow separation prevention and maximum pressure decreases, the initial burn area increase adds many important benefits. First, the range of payloads the sounding rocket can carry increases. The maximum pressure in the case corresponds to maximum thrust and subsequently maximum acceleration. Certain payloads can only experience so many g's to function properly. By reducing the maximum acceleration, a larger range of payloads can be carried by the sounding rocket. Second, the burn profile becomes more neutral/regressive in nature. The ambient pressure for a sounding rocket trajectory is regressive (shown in Fig. 4). For maximum efficiency and altitude, the thrust profile must match the shape of the ambient pressure curve as precisely as possible; another reason to avoid the internal burning tube design since its thrust profile is exactly opposite of Fig. 4. Third, and most importantly, the average pressure in the case increases. Increasing the start-up pressure in the chamber, without affecting the maximum pressure, will increase the average pressure in the case. Since average pressure corresponds

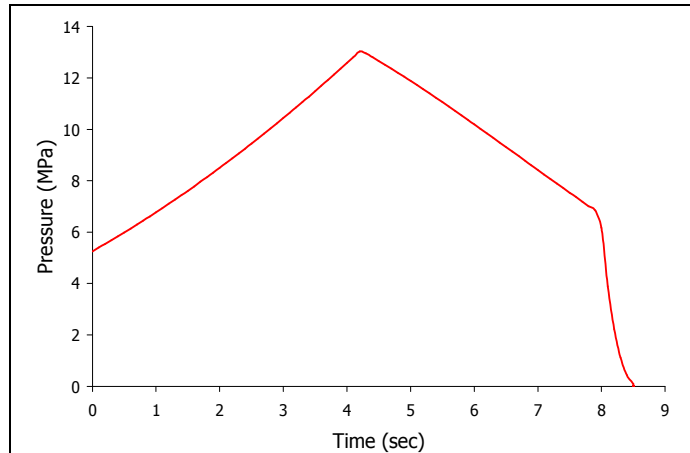


Figure 3. Double Taper Chamber Pressure Profile.
Start-up pressure: 5.25 MPa; max pressure: 13.0 MPa

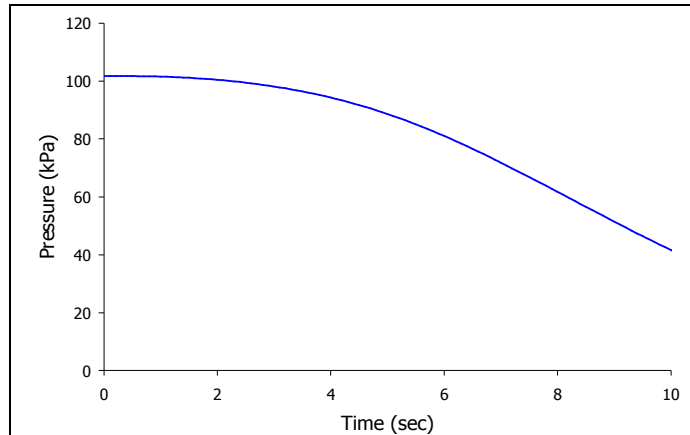


Figure 4. Ambient Pressure Curve for a Sounding Rocket Trajectory

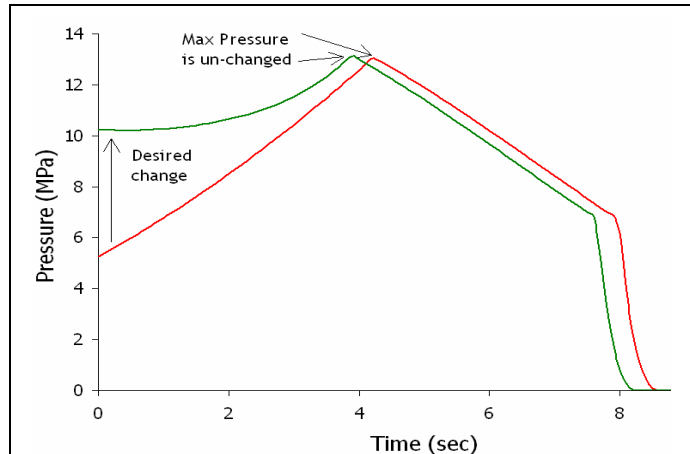


Figure 5. Desired Change in Chamber Pressure Profile

to Isp, increasing the initial burn area will increase the specific impulse of a rocket. Fig. 5 shows the desired effect of increasing the burn area.

The addition of a star design will achieve the desired pressure profile without sacrificing propellant. Fig. 6 provides an example of what a star design will look like when looking down the aft-end of the grain. Notice how the star protrudes inward while adding extra surface area. The protrusion of the star adds propellant to the case rather than sacrificing it like the double taper. As the burns progresses the points of the star will burn away while the grain itself expands. This results in a neutral burn. Combined with the double taper design, a neutral-regressive burn can be produced to maximize the efficiency and improve the altitude of a sounding rocket. It will be demonstrated later that the star grain configuration not only adds more initial surface area than the double taper, but also out-performs the internal burning tube grain design while not exceeding pressure limits.

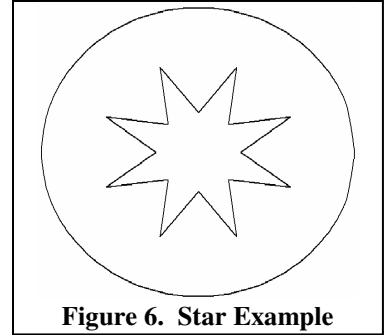


Figure 6. Star Example

III. Star Propagation

To successfully create a model of the star grain configuration, the star must be propagated through time. Because the exact burn rate of a particular propellant is not constant, the star design must propagate as a function of web. Once the star has been successfully propagated, the burn area can be calculated.

A. Propagate the Star Through web

First, set up a definition system for each point of the star. Fig. 7 shows a four pointed star example.

Each star point is comprised of 3 points and two lines. The points are designated by number (1, 2, 3, etc.) and each line is designated with quotation marks ("1", "2", etc.). The reason lines are used is for an easy propagation scheme (described later). Next is a key definition scheme: the $L1$ and $L2$ parameters. $L1$ defines how deep the point drives into the grain and $L2$ defines the width of the star point. These two parameters will define the size and shape of each point of the star and will also be used later to determine the burn area of the star. The W Fig. 7 is the web distance burned. Note the web always burns perpendicular to any surface on the grain. The outside of the circle is the grain to which the star is attached.

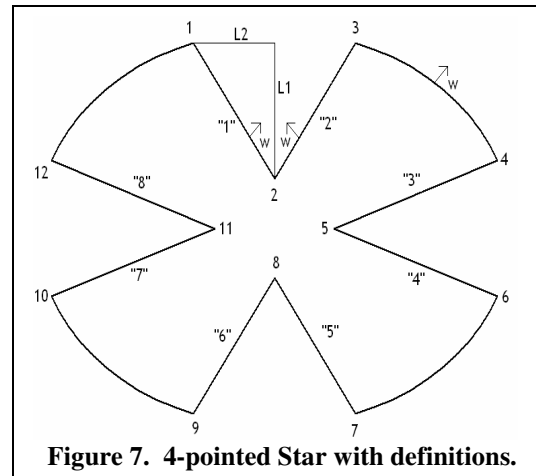


Figure 7. 4-pointed Star with definitions.

The $L1$ and $L2$ parameters will be used to determine the initial parameters of the star. Each line will be defined based on a set coordinate system and propagated through web. Once the location of each point has been determined, from the location of each line, the $L1$ and $L2$ parameters will be re-calculated to calculate a burn area. This will continue until the star design has completely burned away.

For this illustration, only one star point will be propagated. Once modeled, the burn area is just the remainder of star points multiplied by the area discussed here. This star point is the point comprised of points 1, 2, and 3 and lines "1" and "2". Before any math can be involved, an axis system is introduced. The origin is at the center of the star or down the center of case as shown in Fig. 8.

The propagation scheme will utilize the two lines moving together and the outside circle moving outward as a function of web. The intersection of each line with the edge of the circle will denote points 1 and 3 and the intersection of the two lines will denote point 2. To accomplish this, three parameters are needed. The first two are the slope and y-intercept of a line and the third is the radius, R , of the circle. Each line is defined by its slope, m , and its y-intercept, b . Actual equations for each line's respective m and b will come later.

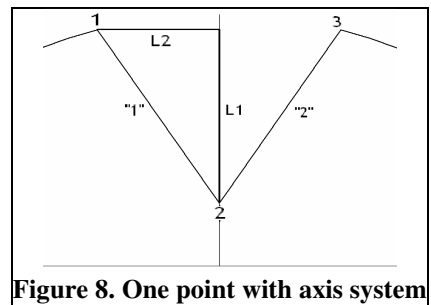


Figure 8. One point with axis system

Each point is determined using a system of equations and solving for their respective x and y coordinates. First, the location of points 1 and 3: these points are located at the intersection of a line and the circle. Eq. (1) represents the equation of a line and Eq. (2) is the circle with radius R .

$$y = mx + b \quad (1)$$

$$y = \sqrt{R^2 - x^2} \quad (2)$$

Set (1) and (2) equal to each other and solve for x. With the aide of the quadratic equation and simplifying techniques, x becomes:

$$x = \frac{-2mb \pm \sqrt{m^2 R^2 - b^2 + R^2}}{2m^2 + 2} \quad (3)$$

Eq. (3) is a very important equation since it defines the most complex point to determine. The +/- sign can be a little tricky. To determine when each sign should be used, look at Fig. 8. “-“ is used for point 1 and “+” is used for point 3. y is determined by using Eq. (1) now that x is known.

Point 2 is determined by solving both Eqs. (4) and (5) (intersection of lines “1” and 2”):

$$y = m_1 x + b_1 \quad (4)$$

$$y = m_2 x + b_2 \quad (5)$$

Solving for the x component yields:

$$x = \frac{b_2 - b_1}{m_1 - m_2} \quad (6)$$

-y is found using either Eqs.(4) or (5) by subbing in the x value found in Eq. (6).

The slope (m) for each line is fairly easy to determine through inspection. The equations are as follows:

$$m_1 = -\frac{L1}{L2} \quad (7)$$

$$m_2 = \frac{L1}{L2} \quad (8)$$

The intercept (b) is slightly more complicated. This requires both inspection and mathematical manipulation. Use the equation of each respective line, Eq. (4) and Eq. (5), and circle, Eq. (2), to compute. Using inspection, x is equal to -L2 for point 1 +L2 for point 3. Solve the equations simultaneously to find each line’s respective b value.

$$b_1 = \sqrt{R^2 - L2^2} - m_1(-L2) \quad (9)$$

$$b_2 = \sqrt{R^2 - L2^2} - m_2(L2) \quad (10)$$

The next step is to propagate each line as a function of web. To accomplish this, it is assumed the line will move along a line normal to itself. The slope of the line will remain the same while the y-intercept will change. Fig. 9 gives a depiction of how this change in b, Δb, is determined using geometry.

The web distance burned, W, forms a right triangle with the initial “1” line, the future “1” line, and the y-axis. Geometry can be used to

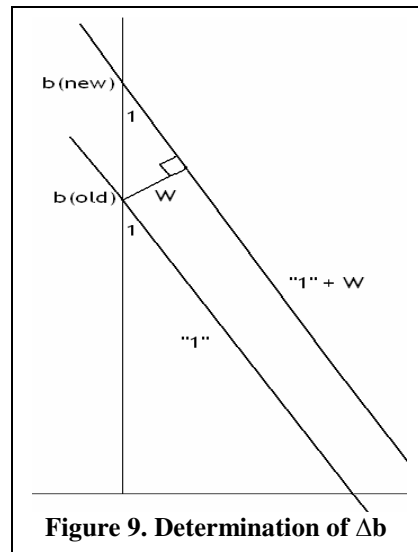


Figure 9. Determination of Δb

determine the distance between the old b and the new b (Δb). Since the slopes of both lines are the same, the angles symbolized as 1 are exactly the same.

$$\theta_1 = \tan^{-1}|m_1| \quad (11)$$

$$\theta_1 = \tan^{-1}\left(\frac{L2}{L1}\right) \quad (12)$$

Solving for Δb :

$$\Delta b = \frac{W}{\sin(\theta_1)} \quad (13)$$

Eq. (13) can be used to propagate both lines “1” and “2”. The equation makes sense theoretically since the y-intercept of both points will move at exactly the same rate and move up (positive y-direction). The star decreases in size over time and will eventually disappear as it moves closer to the main grain. In addition, the intersection of the two lines should not deviate left or right, but should move straight up the y-axis as web is increased.

The simulation of the points is complete. All the initial m 's and b 's have been determined as well their rate of change. By using web, the new slope and y-intercepts of lines “1” and “2” can be determined. The new R is updated using a separate simulation used to propagate the main propellant grain since the radius, R , will change at a different rate depending on what type of grain geometry is used. Once the new m , b , and R have been determined, the points 1, 2, and 3 can be found by using Eqs. (3) and (1) to find the x and y coordinates, respectfully. Through the use of Microsoft Excel, the following simulation of points 1, 2 and 3 propagated through web is shown in Fig. 10.

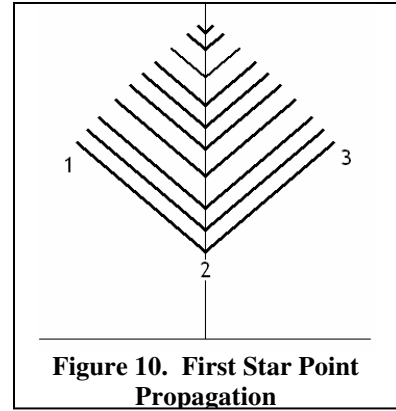


Figure 10. First Star Point Propagation

The point is propagated exactly as expected. The outsides of the point (points 1 and 3) converge on the y-axis at exactly the same rate and point 2 flows up the y-axis. The whole star point diminishes in size while burning along with the main propellant grain.

Now that a working simulation of the star points is verified, the new $L1$ and $L2$ points can be determined. Looking to Fig. 8, the $L1$ and $L2$ points can be found by inspection.

$$L1 = y_1 - y_2 \quad (14)$$

$$L2 = x_3 \quad (15)$$

The subscripts of each x or y correspond to its respective point (i.e. y_1 = the y component of point 1) on Fig. 8. This same process can be used to determine the propagation scheme for the remaining three star points, but each point will propagate exactly the same since the same $L1$ and $L2$ parameters will be used for each star point.

B. Burn Area Calculations

There are two areas to be calculated in this section. The first is an area calculation for a double taper grain design and the second is for an internal burning tube design. The double taper design is the current grain design for the FalconLAUNCH V motor. Thus, the star design was integrated into the double taper design for comparison purposes. Additionally, an internal burning tube star pattern was simulated as another design option.

There are three main components to compute to determine the total area of the burn for a star design. First is the area along the side of star which exists along the main propellant grain. Second is the aft-end section of the star, assuming one aft end is burning along with the main section. Third is an area loss since the star will be taking the place of a once present section on the main propellant grain (this is the area between points 1 and 3 in Fig. 8).

There are three key parameters needed to determine the area of the burn the star design creates. These are the $L1$ and $L2$ parameters as well as the length of the star which runs along the main propellant grain, denoted as Ls .

For the double taper design, the star will only be present in the aft section of the double taper since the forward section does not have enough open space for a star design to really add any performance. Also, the L/D for the forward section is already close to 20, which is a rule of thumb to mitigate the risk of erosive burning. The addition of a star pattern in the forward section could push the L/D over 20, causing erosive burning. Fig. 11 gives a visual of where the star exists in the double taper grain design.

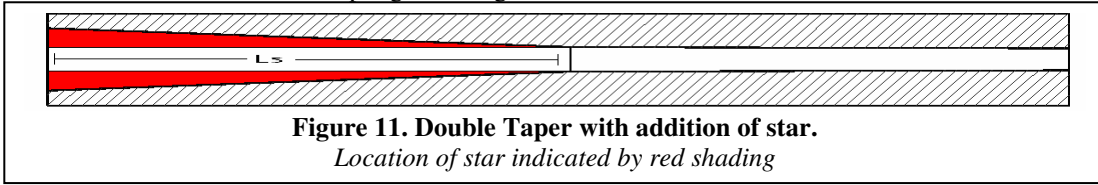


Figure 11. Double Taper with addition of star.
Location of star indicated by red shading

For the internal burning tube grain design, the star will be present for the entire length of the grain. Fig. 12 gives a depiction of the placement of the star for the internal burning tube design.

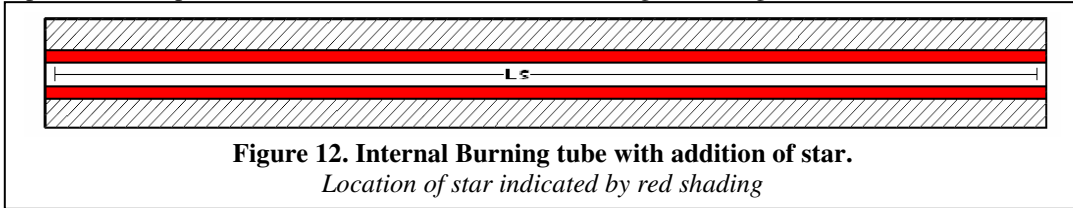


Figure 12. Internal Burning tube with addition of star.
Location of star indicated by red shading

Since $L1$ and $L2$ parameters have already been determined by using the propagation scheme mentioned earlier, the only remaining parameter needed is Ls . The Ls for the internal burning tube design is simple: it is the same as the length of the grain (substitute the length of the grain from the main simulation for Ls). The Ls for the double taper design is much more complicated. As the star burns, the Ls with respect to the aft length of the main grain becomes smaller. Compare Fig. 13 to Fig. 11 to visualize this.

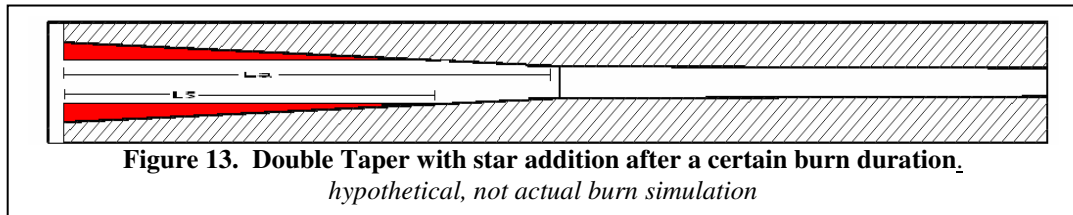


Figure 13. Double Taper with star addition after a certain burn duration.
hypothetical, not actual burn simulation

The Ls term here is significantly less than the aft section of the grain. To find this new Ls term, another determination of points method similar to the one used in the star propagation will be used. The line that is Ls will move towards the grain as the burn progresses. Therefore, the point where the line that is Ls intersects with the main propellant grain is the point used to determine Ls . This point is defined as y_{n2} to be distinguished from y_2 mentioned in the star propagation. The same process used earlier will be used again, except this time the x -coordinate is already known. The y_2 coordinate from the star propagation simulation is the x -coordinate used in Eq. (16). The m and b have already been determined in the main propellant simulation; they are the m and b which describe the line of the aft section of the grain for the double taper design.

$$y_{n2} = m_a y_2 + b_a \quad (16)$$

- Where: $m_a \Rightarrow$ slope of the aft section line
- $b_a \Rightarrow$ y -intercept of the aft section line
- $y_2 \Rightarrow$ y -coordinate of point 2 from Fig. 2

Once this point is determined, subtract it from the aft end of the main propellant grain to find the L_s term.

$$L_s = y_{n2} - y_a \quad (17)$$

- Where: $y_a \Rightarrow$ location of furthest aft section of the grain

The first section to be calculated is the long section of the star which runs along the side of the main propellant grain. This is the section of the star visible in Fig.'s 11, 12 and 13. First, the calculation for the double taper design. By looking at Fig. 11, the area along the long section of the grain forms a triangle. The short end of this triangle is line "1" mentioned in the star propagation section (reference Fig. 8). The long section of the triangle is L_s . Because of the choice to use the parameters $L1$ and $L2$ to describe the shape of the star, the area calculations become simplified. The length of line "1" in Fig. 2 is shown in Eq. (18). Knowing the area of a triangle is $\frac{1}{2}bh$, the area of the long section of the star is Eq. (19).

$$"1" = \sqrt{L1^2 + L2^2} \quad (18)$$

$$A_{LS} = \frac{1}{2} \sqrt{L1^2 + L2^2} L_s \quad (19)$$

This equation describes the burn area for only one section of one star point. There are two sections of burn area per star point. Therefore, Eq. (19) must be corrected to factor in the additional star points and sections. The term *cuts* will be used to designate how many star points exist in the star pattern.

$$A_{LS} = cuts * \sqrt{L1^2 + L2^2} L_s \quad (20)$$

-Where: *cuts* => number of star points in the star pattern

The internal burning tube design is the same, except the area is a rectangle eliminating the $\frac{1}{2}$ term in Eq. (19).

$$A_{LS} = 2 * cuts * \sqrt{L1^2 + L2^2} L_s \quad (21)$$

Next is the end burning section of the star. This area calculation is fairly intuitive looking at Fig. 14.

There are two sections to this calculation: the first is the triangle (colored gray) and the second is the ellipse (colored red). Again, because $L1$ and $L2$ were chosen to define the star point, the area calculations are simple.

The area of the triangle is very simple using the $L1$ and $L2$ parameters. The area of half of the triangle section shown in Fig. 8 is computed using Eq. (22) while the entire end section burn is in Eq. (23):

$$A_{tri} = \frac{1}{2} (L1)(L2) \quad (22)$$

$$A_{tri} = cuts * (L1)(L2) \quad (23)$$

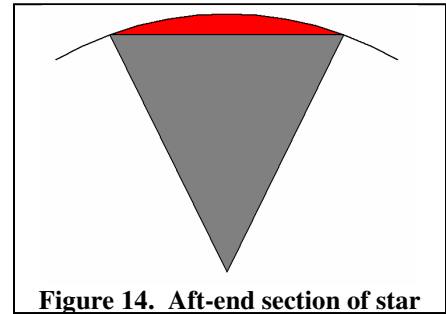


Figure 14. Aft-end section of star

The ellipse can be a bit difficult. The area of an ellipse is $\pi * (ab)$ and is depicted in Fig. 15. The difficult part is finding a and b . a is found by inspecting Fig. 8 and comparing that to the definitions found in Fig. 2. a is $L2$. b is a not as intuitive. Since the y -coordinate of point 1 (Fig. 2) is known and the radius of the circle, R , is known, the difference between them is b . $b = R - y_1$. The area of the ellipse represented in Fig. 8 is only half of an ellipse and each star point has one ellipse section. Therefore, the final equation becomes:

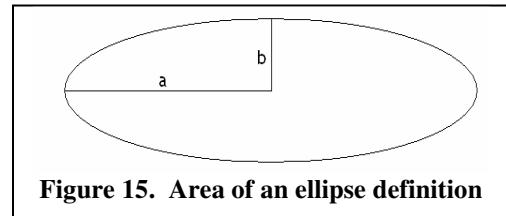


Figure 15. Area of an ellipse definition

$$A_{\text{ellipse}} = \frac{\text{cuts}}{2} L2(R - y_1) \quad (24)$$

Next, the loss of area. The goal is to find the arc length lost and convert this into a total percentage lost along the grain. Fig. 16 provides the relation between the arc length and the parameters $L1$ and $L2$.

To determine the arc length, the unit circle is used to find the actual theta which defines the amount of area lost. Using a scaling factor to size radius of the circle to 1, the following arc length is determined using $L2$ and R :

$$\theta = \sin^{-1}\left(\frac{L2}{R}\right) \quad (25)$$

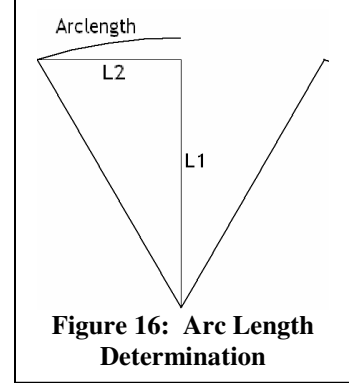


Figure 16: Arc Length Determination

There are two of these thetas per star point and there are 2π radians in a circle. Dividing all the thetas added together by 2π will yield an area loss. For the double taper, do not forget the star is only present in the aft section of the grain. This means there is a $\frac{1}{2}$ factor which needs to be accounted for because the star dwindles down to nothing at the middle part of the grain. Additionally, as the star burns away, the L_s term becomes smaller than the aft length of the grain. This makes the percentage lost along the main grain even less by a factor of L_s/L_a (L_a being the aft length of the grain). Eq. (26) describes the double taper area loss whereas Eq. (27) will describe the area loss for the internal burning tube grain design.

$$\% \text{ gone} = \frac{\text{cuts} * \theta}{2\pi} * \frac{L_s}{L_a} \quad (26)$$

$$\% \text{ gone} = \frac{\text{cuts} * \theta}{\pi} * \frac{L_s}{L_a} \quad (27)$$

IV. Results

After the propagation and area calculations are complete it is time to add the star to a burn simulation and analyze the results. To add the star design to the burn simulation, simply add the additional burn area a star adds to the overall burn area. The two key parameters analyzed will be volumetric efficiency and average chamber pressure, which is related to specific impulse. The overall goal is to maximize total impulse and subsequently altitude.

The baseline grain design used for comparisons is the flight design for FalconLAUNCH V. The flight design is a double taper to take advantage of the initial burn area while not exceeding maximum pressure limits. Three different star grain configurations will be used to compare performance with this baseline grain. The first is an internal burning tube design with a 10-point star pattern embedded throughout the length of the grain. The second two are double taper designs with a star embedded into the aft section of the grain (reference Fig. 11). The first of the double taper/star designs is the same as the baseline motor, but with a 10-pointed star embedded designed to maximize total impulse. The second double taper/star design is the same as the baseline motor, but the aft radius has been increased by .3 in. A 10-point star is then added and optimized to maximize total impulse. The three grain designs will be compared against each other to determine which thrust profile obtains the most altitude. Fig. 17 shows the thrust profiles of the baseline motor and the three star designs. One key thing to notice is the green plot is a neutral-regressive burn. It was mentioned earlier why a neutral-regressive burn is desired and that a star grain configuration could achieve a neutral-regressive burn. This plot verifies the possibility of a neutral-regressive burn using a star pattern.

The lowest performing of the three star grain configurations is the internal burning tube grain design. The two double taper designs out-performed the internal burning tube star grain in every major category. Table 1 summarizes the performance of each grain design while Table 2 summarizes the flight predictions.

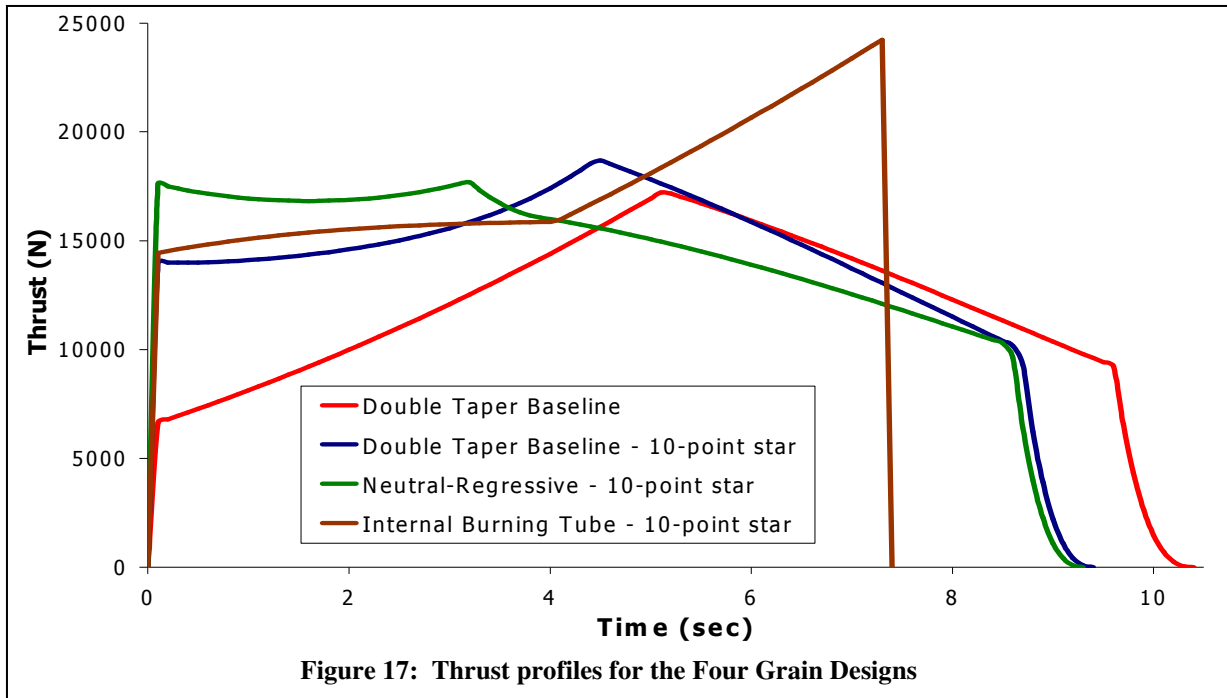
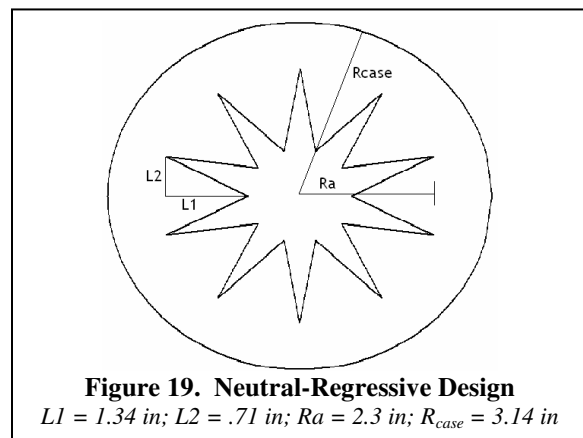
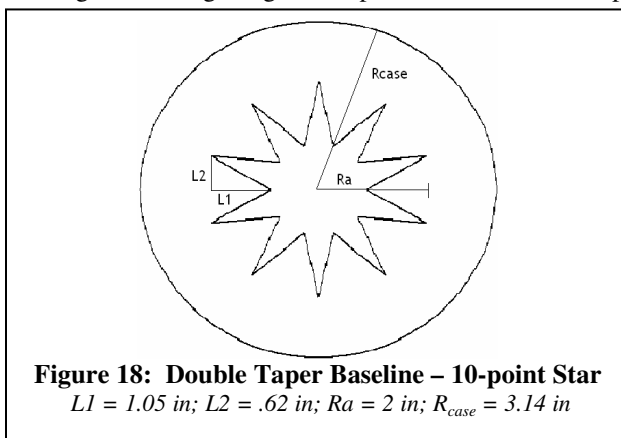


Figure 17: Thrust profiles for the Four Grain Designs

Grain Design	Vol Efficiency (%)	Isp vac (sec)	Total Impulse (N-sec)
Baseline	85.71	266.03	120054
Double Taper Baseline – 10 point star	91.65	269.44	129940
Neutral-Regressive – 10-point star	91.22	269.86	129555
Internal Burning Tube – 10-point star	88.70	269.38	127448

Grain Design	Max Pressure (MPa)	Altitude (km)	Max g's
Baseline	7.76	64.57	26.704
Double Taper Baseline – 10 point star	9.32	89.89	28.423
Neutral-Regressive – 10-point star	9.39	91.90	25.140
Internal Burning Tube – 10-point star	8.33	67.89	71.833

The flight results were generated using the TAOS program using an input thrust profile and mdot simulation. Fig. 18 and Fig. 19 give a depiction of what the star pattern will look like with dimensions added.



The neutral-regressive grain design produced the best flight performance of any grain design; proving it is the most desirable profile to have. Not only did the neutral-regressive burn generate the most altitude, but also endured the lowest max g load. This is due to the neutral-regressive burn giving most of its thrust in the early stages of the burn, since the most mass exists in the rocket at the beginning of the burn. In direct opposition, the internal-burning tube design performed poorly compared to the neutral-regressive design. The internal burning tube grain design produced similar performance numbers when compared to the neutral-regressive. However this is a sounding rocket going to altitude, so the results that really matter are the flight results. The neutral-progressive nature of the internal burning tube is in exact opposition of the desired neutral-regressive profile. Not only did the internal burning tube design fail to make any significant improvements in altitude, but the maximum acceleration felt by the rocket is catastrophic. The internal burning tube design generated more than 70 g's of acceleration. Not only does this mean a payload can't be flown, but the rocket may not even structurally survive the launch without heavier materials to reinforce the structures. The star grain configuration will not only allow the rocket to survive the launch, but will expand the range of possible payloads by lowering the maximum accelerations produced while maximizing altitude.

If max g's are a significant problem, the star design produces so much initial pressure due to the initial burn area present that the throat can be expanded to reduce the total max pressure inside the case. While this will decrease efficiency due to average pressure loss, the maximum pressure and max g load have been decreased significantly. Also, a nearly neutral burn is also possible to bring the maximum pressure down even further. Fig. 20 is a plot of a low g star option. This design only gets to 61 km, but the max g load is only 18.1. The star grain configuration is very versatile in terms of the types of thrust profiles it can produce to achieve a mission.

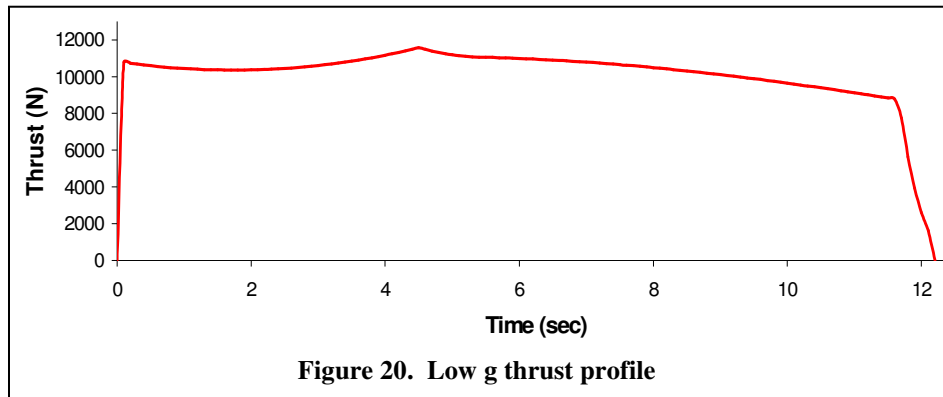


Figure 20. Low g thrust profile

The star grain configuration also avoids flow separation in the nozzle. It was motioned earlier the exit pressure must be above 37 kPa to avoid flow separation. Using the neutral-regressive design with an ideal nozzle and an initial chamber pressure of 9.39 MPa, the initial exit pressure is 89.7 kPa. This is easily above the 37 kPa requirement. In addition, the minimum exit pressure throughout the burn is about 50 kPa at the end of the burn. The star grain configuration avoids flow separation in the nozzle for the duration of the burn.

V. Conclusion

The star grain configuration gains all the benefits of higher initial burn area without the drawback of sacrificing volumetric efficiency. In most cases, the volumetric efficiency is increased when using a star grain configuration. Also, the star pattern is able to achieve a higher Isp because of a higher average chamber pressure throughout the burn. An increase in both volumetric efficiency and Isp leads to a very large increase in total impulse. From a safety perspective, the star pattern prevents flow separation in the nozzle and reduces the maximum chamber pressure to avoid pressure vessel failures. The reduction in maximum chamber pressure also reduces the maximum acceleration of the rocket; increasing the availability of possible payloads. The final benefit of the star grain configuration is the possibility of a neutral-regressive burn. The neutral-regressive burn profile follows the ambient pressure curve more precisely to achieve maximum efficiency. All these benefits added together maximize the performance and flight characteristics of a sounding rocket.

References

¹ Humble, R. W., Henry, G. N., Larson, W. J., *Space Propulsion Analysis and Design*, 1st ed. – revised, The McGraw-Hill Companies, Inc., New York, 1995, pp. 115-117.